Please cite this article in press as: Esteban-Martín et al., Identification of Fibril-Like Tertiary Contacts in Soluble Monomeric α-Synuclein, Biophysical Journal (2013), http://dx.doi.org/10.1016/j.bpj.2013.07.044



# Identification of Fibril-Like Tertiary Contacts in Soluble Monomeric α-Synuclein

Santiago Esteban-Martín,[†] Jordi Silvestre-Ryan,[‡] Carlos W. Bertoncini,[‡*] and Xavier Salvatella[‡§*]
[†]Joint BSC–IRB Research Programme in Computational Biology, Barcelona Supercomputing Center – BSC, Barcelona, Spain;
[‡]Joint BSC–IRB Research Programme in Computational Biology, Institute for Research in Biomedicine (IRB Barcelona), Barcelona, Spain; and [§]Institució Catalana de Recerca i Estudis Avançats (ICREA), Barcelona, Spain

ABSTRACT Structural conversion of the presynaptic, intrinsically disordered protein α-synuclein into amyloid fibrils underlies neurotoxicity in Parkinson's disease. The detailed mechanism by which this conversion occurs is largely unknown. Here, we identify a discrete pattern of transient tertiary interactions in monomeric α-synuclein involving amino acid residues that are, in the fibrillar state, part of β-strands. Importantly, this pattern of pairwise interactions does not correspond to that found in the amyloid state. A redistribution of this network of fibril-like contacts must precede aggregation into the amyloid structure.

## INTRODUCTION

In many neurodegenerative amyloid-linked human conditions, such as Alzheimer's and Parkinson's diseases, fibril formation proceeds via crucial steps that involve monomer to oligomer transition, oligomer maturation, and amyloid formation (1). Recent studies suggest that a complex structural reorganization of the implicated proteins along this process governs neurotoxicity (2–4). However, the precise nature of this conformational rearrangement remains elusive. In this work, we sought to shed light on the early stages of the amyloid pathway of the intrinsically disordered protein (IDP) α-synuclein (αS), a presynaptic protein involved in Parkinson's disease (5). Recent evidence indicates that in vivo αS may coexist between an aggregation-prone monomeric disordered state, an aggregation-resistant tetrameric helix-rich conformation, a helical vesicle-bound state, and different β-sheet-rich species of prefibrillar and fibrillar nature (6–9). Although the structure of αS fibrils has not been unambiguously determined at atomic resolution due to fibril polymorphism (10), the most accepted model suggests that in its fibrillar state αS monomers adopt an antiparallel in-register five β-strand fold (β1 to β5) with monomer units stacked in a parallel fashion forming the fibril protofilament (11). Such structural plasticity has stimulated research toward the structural characterization of αS, which has now become the prototypical example of an IDP.

Despite being largely disordered in solution, monomeric αS is known to populate collapsed conformations (12–14), which are associated with an increase in the rate of protein aggregation (12,14). Several authors have identified the presence of long-range interactions in the protein that put in contact distant regions of the protein (15–20). Studies of the protein in aggregation-prone conditions suggest that these contacts may play a key role in the control of self-oligomerization (15,20,21). Tertiary contacts are thus a fundamental structural feature of this protein that underlies conversion of αS into a neurotoxic, likely β-sheet rich, conformation. NMR studies of soluble αS in supercooling conditions have demonstrated that the monomeric protein transiently populates β-strand-rich conformations within its fibril-forming domain, as judged by negative secondary Cα and C′ deviations as well as positive secondary 3J(HNHα) couplings (22). No transient tertiary interactions between residues forming β-strands in the amyloid state have yet been described in the monomeric state of the protein; however, close examination of NMR (15–17), single-molecule Föster Resonance Energy Transfer (FRET) (18,19), and electron transfer kinetics data (20) suggest a more complex pattern of transient tertiary interactions in solution than the one identified so far (Fig. 1, *a* and *b*).

Here, we mapped at high resolution this network of transient tertiary interactions present in the soluble monomeric state of αS and found a fingerprint of its amyloid fibrillar structure. To calculate a high-resolution interresidue contact map of αS, we employed an extensive set of intramolecular paramagnetic relaxation enhancement (PRE) data for the monomeric state of the protein (15,16,23,24). PREs are an extremely powerful NMR parameter for detecting long-range transiently formed contacts in IDPs due to the highly nonlinear distance-dependent enhancement of relaxation rates in nuclei induced by the presence of paramagnetic spin probes (25). Our contact map of αS provides novel, to our knowledge, insights into the relationship between the structural properties of amyloid fibrils and those of their monomeric precursors as well as on the conformational changes that would occur during amyloid formation.

## MATERIALS AND METHODS

### Intramolecular PRE data

PRE-derived interresidue distance restraints for αS at pH 7.4 were collected from works published by leading laboratories in the study of the structural

*Submitted March 22, 2013, and accepted for publication July 25, 2013.*

*Correspondence: carlos.bertoncini@irbbarcelona.org or xavier.salvatella@irbbarcelona.org

Editor: Josh Wand.



0006-3495/13/09/0001/7 $2.00

http://dx.doi.org/10.1016/j.bpj.2013.07.044

Please cite this article in press as: Esteban-Martín et al., Identification of Fibril-Like Tertiary Contacts in Soluble Monomeric α-Synuclein, Biophysical Journal (2013), http://dx.doi.org/10.1016/j.bpj.2013.07.044



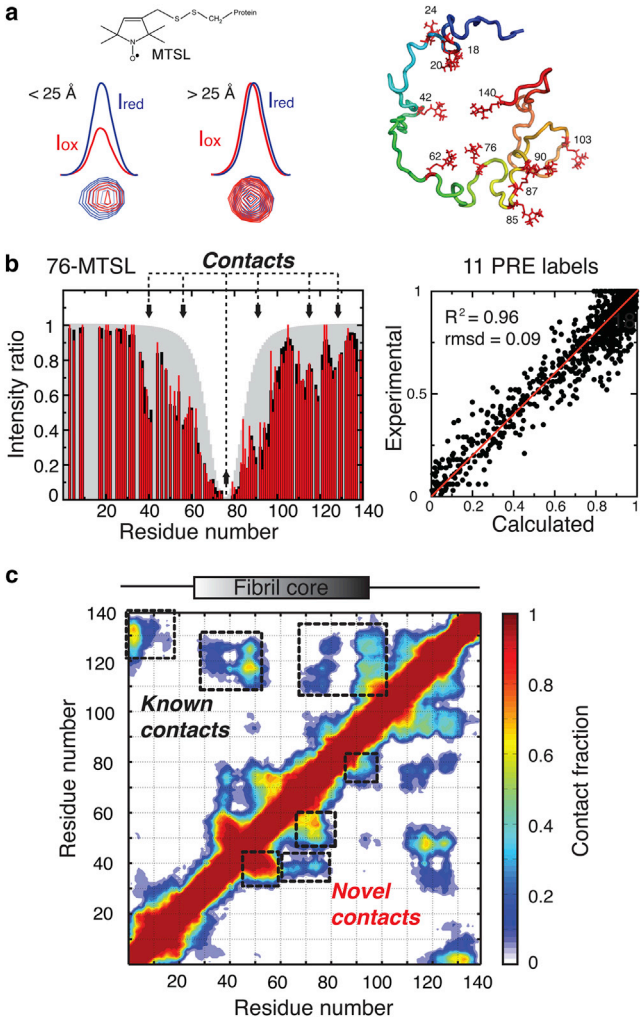


FIGURE 1 High-resolution mapping of tertiary contacts in monomeric αS. (*a*) Spin labeling of single Cys-containing αS variants with MTSL leads to mapping of tertiary contacts by NMR. Nuclei within a distance of up to 25 Å from the PRE label suffer attenuation of its NMR intensity, which is proportional to $r^{-6}$. Positions of PRE labels used in the structure calculations are shown in red. (*b*) Left panel: Experimental PRE data (*red*) and fitted PRE data (*black*) are shown for a representative position of the MTSL label (76-MTSL). The expected profile for a random coil is shown in gray. Tertiary contacts are highlighted by arrowed dashed lines. Right panel: Results of the structure calculation procedure that best fit the data. Forty independent calculations were performed and the structures were pooled before contact map analysis. (*c*) Interresidue Cα-Cα contact map resulting from the structure calculations. Contact fraction denotes the number of conformers from the pool that contain a given contact. Contacts previously reported in the literature are highlighted as *Known* contacts (15,16,20). Contacts discovered in this work are highlighted as *Novel* contacts.

properties of this protein (see Table S1 in the Supporting Material) (15–17,23). In total, we analyzed 1104 intensity ratios arising from 11 spin probes (MTSL: (*S*-(2,2,5,5-tetramethyl-2,5-dihydro-1H-pyrrol-3-yl)methylmethanesulfonothioate) located at various positions along the polypeptide chain (amino acids 18, 20, 24, 42, 62, 76, 85, 87, 90, 103, and 140). Under these experimental conditions of low temperature and low concentration, αS remains monomeric and no oligomerization is detectable by any ensemble spectroscopic method or by control intermolecular PREs experiments employing mixtures of PRE-tagged $^{14}N$ protein and untagged $^{15}N$ protein (16). Because of this experimental setup, we can be confident that PRE effects arise predominantly from intramolecular interactions, however we cannot completely rule out a marginal contribution of intermolecular nature arising from transient low order oligomeric species (26) (see discussion in the Supporting Material). A scaling factor had to be introduced in the case of some PRE labels to compensate for slight variations in experimental conditions between data sets, temperature, and reduction of the MTSL label. Scaling factors were determined by normalization of each data set to their respective average values. Scaling factors applied were 1.17 for labels at positions at 18, 90, and 140 (15); 1.25 for labels at positions 20 and 85 (17); 1.0 for positions 24, 42, 62, 87, and 103 (16); and 1.0 for the label at position 76 (23).

## Determination of contacts maps

Structure calculations were performed using full-atom Monte Carlo (MC) simulations guided by PRE experimental restraints (27) (see extended details in the Supporting Material, Supplementary data). The calculation method was benchmarked with synthetic PRE data generated for the protein αS, as well as other intrinsically disordered and chemically denatured proteins (27). PRE intensity ratios on HN atoms (intensity ratio between $^{1}H$-$^{15}N$ amide crosspeaks in oxidized and reduced states of the spin label) were calculated at each MC move. The MTSL spin label was explicitly built and rotated at each step to sample the accessible conformational space. Calculations were performed for ensembles sizes of 1, 2, 5, 10, 20, and 50 conformers (see Fig. S4). The calculation procedure was repeated 40 times for each ensemble size and structures were pooled before contact map analysis. For ensemble size 1 (7.8 restrains/amino acid), data were fitted within experimental error ($R^2$ = 0.96, root mean-square deviation (rmsd) = 0.09). Only a marginal increment in the goodness of the fit was obtained for ensemble sizes larger than 1 (Δrmsd = 0.01). As shown before, due to the $r^{-6}$ weighted averaging of the PRE effect, employing a limited number of conformers to satisfy the PRE distance restraints avoids the presence of unrestrained conformers (28). Energy minimization of the structures determined using the AMBER force field in GROMACS (29) left the calculated structures virtually unchanged. Cα-Cα contact maps were generated averaging 40 structures obtained from independent runs, which formed a well-defined cluster of conformations. A contact was defined as a Cα-Cα interresidue distance up to 20 Å (range of PRE action). The contacts reported for the fibril correspond to ssNMR data previously reported (11). This data considers contacts between residues within 6 Å, which have been extracted from 13C–13C proton-driven spin diffusion spectra (experiment with a mixing time of 250 ms).

## Physicochemical characteristics of the primary sequence of αS

Data were generated using the Expasy protscale server (http://web.expasy.org/cgi-bin/protscale/protscale.pl). Hydrophobicity at pH 7.5 obeys the scales reported by Cowan et al (30). A sliding average window of seven residues was employed. The profile of predicted amyloid aggregation follows the commonly used algorithms WALTZ (high sensitivity filter) and Zyggregator (Zagg) (31,32).

## RESULTS

As a starting point in our calculations, we collected a large set of intramolecular PRE data from 11 paramagnetic labels previously measured for monomeric αS under conditions that minimize the presence of oligomeric species (pH 7.4, 100 μM protein concentration, temperature of 10 to

Please cite this article in press as: Esteban-Martín et al., Identification of Fibril-Like Tertiary Contacts in Soluble Monomeric α-Synuclein, Biophysical Journal (2013), http://dx.doi.org/10.1016/j.bpj.2013.07.044



15°C). To ensure coherency between the data sets we implemented a scaling factor (Table S1). Thus, our calculation strategy employs a total of 1104 distance restraints, two to three times the number of PRE restraints used in previous analysis of the protein (15,16,23,24). The interresidue contact map was derived by fitting the PRE data to structural models by using a full-atom MC structure calculation method that we recently developed (27) (Fig. 1 *c*, Fig. S1, and Supplementary data). It is important to clarify that αS populates an ensemble of rapidly interconverting conformations in solution and, therefore, the interresidue contact map is a projection of all tertiary interactions, populated up to a few percent by the disordered state of the protein, some of which may not be simultaneous.

The interresidue contact map we determined for αS highlights with unprecedented detail previously known long-range interactions between the C-terminus of the protein with both the N-terminal and central parts of the protein, termed NAC (Fig. 1 *c*, *Known contacts* and Fig. S3) (15,16,20). We find that the C-terminal region possesses a strong avidity for establishing interactions: the region $_{124}$AYEMPSEEGYQDYEP$_{138}$ contacts residues $_{1}$MVDFMKGLMK$_{10}$, whereas the region comprising residues $_{104}$EEGAPQEGILEDMPVDPNEAYEMPSE$_{130}$ interacts with three segments involving residues $_{38}$LYVGSKTKEGVVHGVATVA$_{56}$, $_{74}$VTAVAQK$_{80}$, and $_{90}$AATGFVKKDQL$_{100}$. The charged nature of these regions underlies their contact tendency.

Due to the high resolution achieved in our calculations, a number of short-range contacts could also be resolved indicating a strong degree of collapse present at both the N- and C-terminal regions of the protein (Fig. 1 *c*). At the N-terminus, the collapsed state spans up to residue 30, which could reflect the population of conformations with nascent helical content because this region folds into an α-helix upon oligomerization or in the presence of phospholipids (33). Indeed, studies of $^{15}$N relaxation and secondary chemical shifts indicate partial population of helical conformations by this domain in the momomeric state of the protein (34,35). The collapse at the C-terminus is centered on residue 120, the region with the highest degree of residual structure in the protein, as judged by unusually high NMR residual dipolar couplings (15), and being also a major metal binding site (36).

Most notably, our high-resolution contact map reveals an up to now unreported pattern of transient tertiary interactions in αS (Fig. 1 *c*, *Novel contacts*, Fig. S3). A comparative analysis with ssNMR data measured for αS fibrils indicates that these contacts involve amino acids that form the β-strands within the amyloid fibril core of αS (β1 to β5), therefore we termed these as fibril-like contacts (Fig. 2, *a* and *b*). In Fig. 2 we compare the tertiary contacts found in solution with contacts derived from the ssNMR model of the fibril. According to ssNMR, H/D exchange mass spectrometry and electron paramagnetic resonance

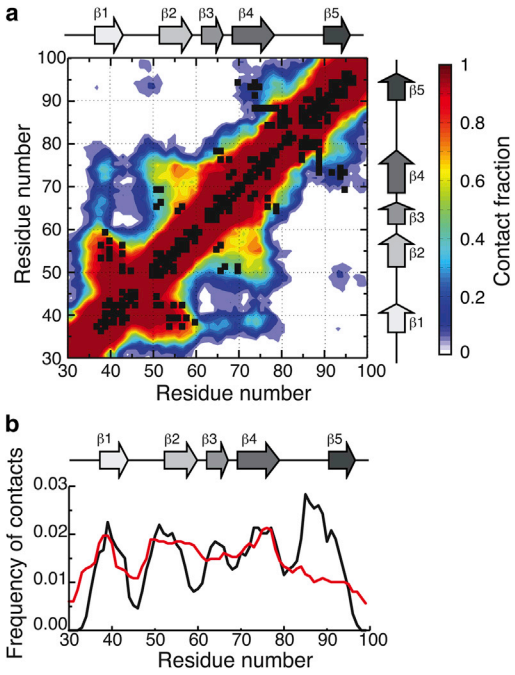


FIGURE 2 Fibril-like contacts are present in soluble monomeric αS. (*a*) Overlay of contacts determined by ssNMR in the amyloid core of αS fibrils (*black dots*) with fibril-like contacts described for soluble αS in this work. β-strands found in the fibrillar core are depicted as grayscale arrows numbered 1 to 5. (*b*) Frequency of contacts established by residues within the amyloid core of αS in its soluble state (*red line*) and in the fibril (*black line*). Contacts established by residues of the region 30–100 are considered in this analysis.

data, the amyloid core of the fibril comprises, approximately, residues 30 to 100 (11,37,38). Therefore, we decided to focus our analysis on this stretch of residues. From this figure it is noteworthy that, although some of these fibril-like interactions correlate directly with contacts established in the amyloid fold of αS, referred here as *fibrillar contacts*, the remaining establish a mismatched pattern of pairwise interactions respect to the arrangement found in its amyloid state, referred herein as *nonfibrillar contacts* (Fig. 2 *a*, Fig. 3 *a*). Among the fibrillar contacts, we were able to resolve tertiary contacts between β1–β2 and β4–β5, two fibril-like interactions that could seed amyloid conversion. We cannot exclude contacts between β2–β3–β4, which are likely to occur, but could not be resolved due to the short-range nature of these contacts and the presence of overlapping interactions.

As mentioned, we also detected in monomeric αS a pattern of nonfibrillar contacts between residues that are, in the fibrillar state, part of β-strands. The most remarkable of such interactions involves the stretch of residues $_{35}$EGVLYV$_{40}$ contacting residues $_{70}$VVTGVTAVA$_{78}$. These two regions correspond to β1 and β4 strands of the amyloid fibril (Fig. 2 *a*, Fig. 3 *a*) and contain Tyr$_{39}$ and the stretch of hydrophobic residues 71–82, both known to be critical for fibril formation (39,40). We also observed

Please cite this article in press as: Esteban-Martín et al., Identification of Fibril-Like Tertiary Contacts in Soluble Monomeric α-Synuclein, Biophysical Journal (2013), http://dx.doi.org/10.1016/j.bpj.2013.07.044



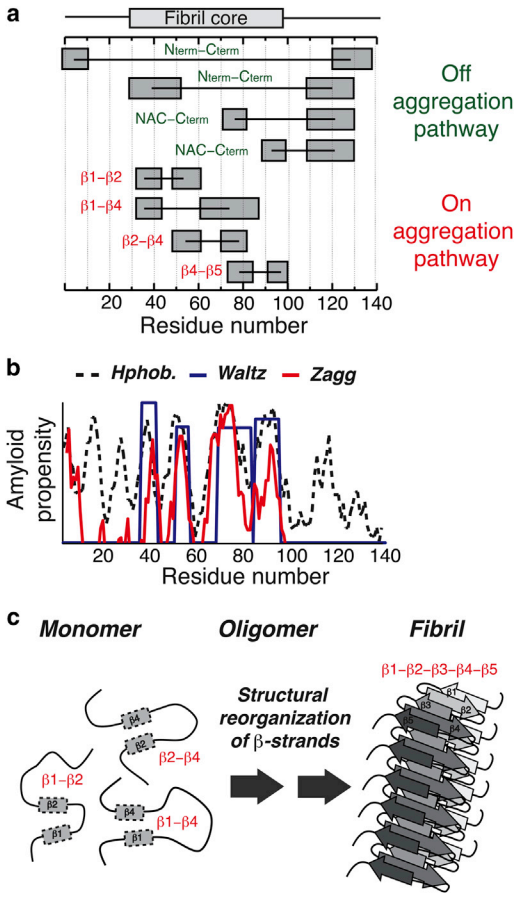


FIGURE 3 Reorganization of contacts between β-strands during aggregation of αS. (*a*) Overview of contacts described for soluble αS in this work. The regions involved in the establishment of each particular contact are identified with green labels if they are off the aggregation pathway (N-terminus, NAC, C-terminus) or with red if they are on the aggregation pathway (strands β1 to β5). (*b*) Fibril-like contacts are established between hydrophobic regions predicted as highly amyloid prone. Predictions for αS aggregation computed by WALTZ (amyloid-forming regions, *blue line*) and Zyggregator (Zagg, amyloid aggregation propensity, *red line*). Hydrophobicity is shown as a black dashed line. (*c*) Our high-resolution contact map for monomeric αS suggests that residues within the fibril-forming domain of the protein adopt a different spatial arrangement in solution than in the fibrillar state, demanding structural reorganization of contacts between residues in β-strands before amyloid formation. Such reorganization would probably take place at the level of oligomeric and prefibrillar species.

nonfibrillar contacts between regions involving residues that correspond to strands β1–β3, β2–β4, and β2–β5 in the amyloid fibril. Nonfibrillar interactions established by these residues are mismatched contacts that would require reorganization before fibril formation, similar to nonnative interactions that modulate the folding of certain globular proteins (41–45).

A close analysis of the nature of the regions involved in establishing fibril-like contacts in soluble monomeric αS indicates that these interactions are of hydrophobic nature and engage residues commonly found in intermolecular complexes involving IDPs (46). Note that these hydrophobic regions form a discrete pattern of contacts instead of an all-to-all interacting pattern, suggesting a complex hierarchy in the establishment of tertiary interactions. Fibril-like contacts appear to be modulated by amino acid regions with a high propensity to aggregate into amyloid fibrils, according to the predictions made by two commonly used algorithms (31,32) (Fig. 3 *b*), and further validated by experimental data (39,40).

## DISCUSSION

The investigation of aggregation-prone conformations populated in the monomeric ensemble of amyloidogenic IDPs such as αS, Tau, or Aβ aims to identify structural elements that could initiate protein misfolding and aggregation in pathologies such as Alzheimer's and Parkinson's. During the last years a large number of research groups have implemented NMR and computational methodologies to characterize such heterogeneous conformations with atomic detail (47). In the absence of persistent secondary structure, one of the primary elements that restrict the conformations populated by IDPs is tertiary interactions, which are detected by NMR methodologies such as PREs (48). With the aim of uncovering low populated contacts that were previously not identified in αS, in this work we characterized tertiary contacts present in the monomeric state of the protein that are consistent with a large set of intramolecular PRE data. Indeed, our contact map allowed us to describe for the first time, to our knowledge, tertiary interactions present in the soluble state of αS that arise from regions of sequence involved in the cross-β core of the fibrils, but that do not correspond to those found in the amyloid state (Fig. 3). Although we positively identified fibrillar contacts between residues forming β1–β2 and β4–β5 strands, we also found nonfibrillar contacts between residues embedded in β1–β4, β1–β3, β2–β4, and β2–β5 strands of the amyloid fibril. Importantly, close examination of the PRE profiles shows that all of these interactions are indeed present in the experimental data and are not a consequence of the structure calculation protocol (Fig. S3).

These findings have mechanistic implications for the current knowledge of the fibrillation pathway of αS. Intramolecular long-range N/C-terminal tertiary interactions in the soluble state of αS have been proposed to maintain the monomeric protein in an autoinhibited, less aggregation-prone conformation (15,16,20). These contacts thus lie off the pathway of amyloid aggregation (Fig. 3 *a*). The transient tertiary contacts between hydrophobic regions participating in the fibril core of the protein would, by contrast, direct the formation of early aggregation-prone species (Fig. 3 *a*). Conceptually related to a folding nucleus, these contacts would lead to the buildup of metastable species rich in cross-β structure but with a network of interresidue interactions different to that of mature fibrils (3,11).

Please cite this article in press as: Esteban-Martín et al., Identification of Fibril-Like Tertiary Contacts in Soluble Monomeric α-Synuclein, Biophysical Journal (2013), http://dx.doi.org/10.1016/j.bpj.2013.07.044



According to our model, initial oligomerization would then be followed by a step where such network reorganizes to lead to the thermodynamically stable 5 $\beta$-strand fold of the amyloid fibril. Spectroscopy studies indicate that initial steps of $\alpha$S aggregation give rise to prefibrillar oligomeric species that have different $\beta$-sheet signatures than mature amyloid fibrils, as judged by ssNMR and FTIR (49,50). In addition, single-molecule FRET studies showed that the structural conversion between oligomeric forms of $\alpha$S into $\beta$-sheet-rich oligomers is remarkably slow and progresses through a rough energy landscape as a result of multiple possibilities of interstrand interactions (3). All this experimental evidence is consistent with our finding that structural signatures of soluble and fibrillar $\alpha$S species would have a different $\beta$-strand arrangement (Fig. 3 *c*). In the broad context of protein misfolding and aggregation, our data suggests that on-pathway oligomeric intermediates may be stabilized by nonfibrillar contacts akin to the nonnative interactions that stabilize certain folding intermediates in globular proteins (41–45). Such nonfibrillar contacts could be crucial for frustrating unspecific amorphous aggregation and facilitating instead well-ordered amyloid aggregation, sustaining the idea of a rugged energy landscape in the misfolding and aggregation of proteins (51). It could be of particular interest to unravel this proposed mechanism experimentally by, for example, enforcing some of these contacts by covalent linkage of Cys-containing mutants of $\alpha$S. Such a procedure was recently applied to the A$\beta$ peptide and yielded very important insights into the earliest stages of aggregation (52). In an analogous fashion it should be possible to isolate and characterize the transient oligomeric intermediates formed by $\alpha$S by stabilizing the nonfibrillar contacts that we discovered in this work.

We note that antiamyloidogenic agents that target monomeric $\alpha$S have been recently shown to interact with $Tyr_{39}$ ($\beta$1) or key hydrophobic residues in the central part of the protein ($\beta$4 and $\beta$5) (39,53–55). Mostly of polyphenolic nature, these agents establish $\pi$-$\pi$ stacking interactions with the side chain of $Tyr_{39}$ and interact in a rather unspecific manner with the stretch of hydrophobic residues comprising amino acids 70–90. In light of our data, it is then possible that such small molecules prevent crucial structural rearrangements to take place at the level of the monomeric protein by inhibiting some of the long-range fibrillar contacts established between residues that compose the $\beta$-strand regions of the fibril. Identification of such regions that are necessary brought together into spatial proximity to set off protein aggregation could facilitate the design of novel, to our knowledge, small molecules that could modulate fibril formation.

The intra- versus intermolecular nature of tertiary N/C interactions provides an increased layer of complexity in the aggregation pathway of $\alpha$S. Here, we mapped with high resolution the intramolecular N/C-terminal interactions occurring at the level of the monomeric protein. Noteworthy, intermolecular PRE studies of partially oligomeric $\alpha$S (1.1 mM protein concentration) showed transient interchain N/C-terminal interactions involving residues 1–15/120–140 and 35–45/120–140, precisely two of the main interactions detected in our contact map of the monomeric protein (26). In this regard, it was previously shown that ligands that bind the C-terminus trigger protein aggregation by release of the intramolecular N/C interactions (15), and more recently fluorescence spectroscopy evidenced local structural reorganization at both the N- and C-termini preceding oligomerization (56). Moreover, measurements of intrachain diffusion rates in $\alpha$S monomers showed that intramolecular reconfiguration of tertiary contacts determines the kinetics of bimolecular association (57). It is then evident that residual structure at both the N- and C-terminus, and its interplay via long-range interactions, appears to govern the early steps in $\alpha$S oligomerization. The possibility of swapping between intra- and intermolecular contacts while remaining disordered offers a rationale for the initial population of oligomeric species in the amyloid pathway of $\alpha$S with minimal energetic costs. Even when these regions are not directly involved in the fibrillar core of the protein, they seem to communicate via intrachain contacts to dictate the conformations populated by the protein. For example, nitration of C-terminal Tyr residues perturbs binding of the N-terminus to lipid membranes via a yet unknown mechanism that could, very likely, involve reorganization at the level of N/C interactions (19).

The unexpected complexity in the nature and functionality of the network of short- and long-range tertiary interactions of monomeric $\alpha$S could have implications for our future understanding of the biological relevance of such transient structural features in IDPs. From this work it is evident that a high-resolution description of tertiary contacts using small ensembles is a very valuable complementary study to the use of large ensembles (47,48,58,59). Although the latter approaches allow a more general description of the vast conformational space populated by the disordered protein, our methodology allows identifying with higher precision biologically relevant contacting regions of the polypeptide chain. In particular, the description of fibril-like interactions in monomeric $\alpha$S could allow better identification and targeting of aggregation-prone species within the ensemble of $\alpha$S conformations.

## SUPPORTING MATERIAL

Six figures, two tables, references (60–64), and supplementary data are available at http://www.biophysj.org/biophysj/supplemental/S0006-3495(13)00866-7.

This work was supported by grants from the EU-FP7 (Marie Curie fellowship to C.W.B.), Institute for Research in Biomedicine (IRB) Barcelona (X.S.), Institució Catalana de Recerca I Estudis Avançats (ICREA) (X.S.), Spanish Ministerio de Ciencia e Innovación (MICINN) (X.S.), and Marató de TV3 (102030). C.W.B. is a holder of a Ramón y Cajal

Please cite this article in press as: Esteban-Martín et al., Identification of Fibril-Like Tertiary Contacts in Soluble Monomeric α-Synuclein, Biophysical Journal (2013), http://dx.doi.org/10.1016/j.bpj.2013.07.044



research contract from MICINN. S.E.M. is a holder of a Juan de la Cierva research contract from MICINN.

## REFERENCES


1. Chiti, F., and C. M. Dobson. 2006. Protein misfolding, functional amyloid, and human disease. *Annu. Rev. Biochem.* 75:333–366.
2. Campioni, S., B. Mannini, …, F. Chiti. 2010. A causative link between the structure of aberrant protein oligomers and their toxicity. *Nat. Chem. Biol.* 6:140–147.
3. Cremades, N., S. I. Cohen, …, D. Klenerman. 2012. Direct observation of the interconversion of normal and toxic forms of α-synuclein. *Cell.* 149:1048–1059.
4. Miller, Y., B. Ma, and R. Nussinov. 2010. Polymorphism in Alzheimer Abeta amyloid organization reflects conformational selection in a rugged energy landscape. *Chem. Rev.* 110:4820–4838.
5. Dawson, T. M., and V. L. Dawson. 2003. Molecular pathways of neurodegeneration in Parkinson's disease. *Science.* 302:819–822.
6. Lashuel, H. A., C. R. Overk, …, E. Masliah. 2013. The many faces of α-synuclein: from structure and toxicity to therapeutic target. *Nat. Rev. Neurosci.* 14:38–48.
7. Bartels, T., J. G. Choi, and D. J. Selkoe. 2011. α-Synuclein occurs physiologically as a helically folded tetramer that resists aggregation. *Nature.* 477:107–110.
8. Fauvet, B., M. K. Mbefo, …, H. A. Lashuel. 2012. α-Synuclein in central nervous system and from erythrocytes, mammalian cells, and *Escherichia coli* exists predominantly as disordered monomer. *J. Biol. Chem.* 287:15345–15364.
9. Karpinar, D. P., M. B. Balija, …, M. Zweckstetter. 2009. Pre-fibrillar alpha-synuclein variants with impaired beta-structure increase neurotoxicity in Parkinson's disease models. *EMBO J.* 28:3256–3268.
10. Heise, H., W. Hoyer, …, M. Baldus. 2005. Molecular-level secondary structure, polymorphism, and dynamics of full-length alpha-synuclein fibrils studied by solid-state NMR. *Proc. Natl. Acad. Sci. USA.* 102:15871–15876.
11. Vilar, M., H. T. Chou, …, R. Riek. 2008. The fold of alpha-synuclein fibrils. *Proc. Natl. Acad. Sci. USA.* 105:8637–8642.
12. Uversky, V. N., J. Li, and A. L. Fink. 2001. Evidence for a partially folded intermediate in alpha-synuclein fibril formation. *J. Biol. Chem.* 276:10737–10744.
13. Morar, A. S., A. Olteanu, …, G. J. Pielak. 2001. Solvent-induced collapse of alpha-synuclein and acid-denatured cytochrome *c*. *Protein Sci.* 10:2195–2199.
14. Lee, J. C., R. Langen, …, J. R. Winkler. 2004. Alpha-synuclein structures from fluorescence energy-transfer kinetics: implications for the role of the protein in Parkinson's disease. *Proc. Natl. Acad. Sci. USA.* 101:16466–16471.
15. Bertoncini, C. W., Y. S. Jung, …, M. Zweckstetter. 2005. Release of long-range tertiary interactions potentiates aggregation of natively unstructured alpha-synuclein. *Proc. Natl. Acad. Sci. USA.* 102:1430–1435.
16. Dedmon, M. M., K. Lindorff-Larsen, …, C. M. Dobson. 2005. Mapping long-range interactions in alpha-synuclein using spin-label NMR and ensemble molecular dynamics simulations. *J. Am. Chem. Soc.* 127:476–477.
17. Sung, Y. H., and D. Eliezer. 2007. Residual structure, backbone dynamics, and interactions within the synuclein family. *J. Mol. Biol.* 372:689–707.
18. Ferreon, A. C., Y. Gambin, …, A. A. Deniz. 2009. Interplay of alpha-synuclein binding and conformational switching probed by single-molecule fluorescence. *Proc. Natl. Acad. Sci. USA.* 106:5645–5650.
19. Sevcsik, E., A. J. Trexler, …, E. Rhoades. 2011. Allostery in a disordered protein: oxidative modifications to α-synuclein act distally to regulate membrane binding. *J. Am. Chem. Soc.* 133:7152–7158.
20. Lee, J. C., H. B. Gray, and J. R. Winkler. 2005. Tertiary contact formation in alpha-synuclein probed by electron transfer. *J. Am. Chem. Soc.* 127:16388–16389.
21. Lee, J. C., B. T. Lai, …, J. R. Winkler. 2007. Alpha-synuclein tertiary contact dynamics. *J. Phys. Chem. B.* 111:2107–2112.
22. Kim, H. Y., H. Heise, …, M. Zweckstetter. 2007. Correlation of amyloid fibril beta-structure with the unfolded state of alpha-synuclein. *ChemBioChem.* 8:1671–1674.
23. Salmon, L., G. Nodet, …, M. Blackledge. 2010. NMR characterization of long-range order in intrinsically disordered proteins. *J. Am. Chem. Soc.* 132:8407–8418.
24. Allison, J. R., P. Varnai, …, M. Vendruscolo. 2009. Determination of the free energy landscape of alpha-synuclein using spin label nuclear magnetic resonance measurements. *J. Am. Chem. Soc.* 131:18314–18326.
25. Clore, G. M., and J. Iwahara. 2009. Theory, practice, and applications of paramagnetic relaxation enhancement for the characterization of transient low-population states of biological macromolecules and their complexes. *Chem. Rev.* 109:4108–4139.
26. Wu, K. P., and J. Baum. 2010. Detection of transient interchain interactions in the intrinsically disordered protein alpha-synuclein by NMR paramagnetic relaxation enhancement. *J. Am. Chem. Soc.* 132:5546–5547.
27. Silvestre-Ryan, J., C. W. Bertoncini, …, X. Salvatella. 2013. Average conformations determined from PRE data provide high-resolution maps of transient tertiary interactions in disordered proteins. *Biophys. J.* 104:1740–1751.
28. Ganguly, D., and J. Chen. 2009. Structural interpretation of paramagnetic relaxation enhancement-derived distances for disordered protein states. *J. Mol. Biol.* 390:467–477.
29. Van Der Spoel, D., E. Lindahl, …, H. J. Berendsen. 2005. GROMACS: fast, flexible, and free. *J. Comput. Chem.* 26:1701–1718.
30. Cowan, R., and R. G. Whittaker. 1990. Hydrophobicity indices for amino acid residues as determined by high-performance liquid chromatography. *Pept. Res.* 3:75–80.
31. Maurer-Stroh, S., M. Debulpaep, …, F. Rousseau. 2010. Exploring the sequence determinants of amyloid structure using position-specific scoring matrices. *Nat. Methods.* 7:237–242.
32. Tartaglia, G. G., and M. Vendruscolo. 2008. The Zyggregator method for predicting protein aggregation propensities. *Chem. Soc. Rev.* 37:1395–1401.
33. Bussell, Jr., R., and D. Eliezer. 2003. A structural and functional role for 11-mer repeats in alpha-synuclein and other exchangeable lipid binding proteins. *J. Mol. Biol.* 329:763–778.
34. Eliezer, D., E. Kutluay, …, G. Browne. 2001. Conformational properties of alpha-synuclein in its free and lipid-associated states. *J. Mol. Biol.* 307:1061–1073.
35. Bussell, Jr., R., and D. Eliezer. 2001. Residual structure and dynamics in Parkinson's disease-associated mutants of alpha-synuclein. *J. Biol. Chem.* 276:45996–46003.
36. Binolfi, A., R. M. Rasia, …, C. O. Fernández. 2006. Interaction of alpha-synuclein with divalent metal ions reveals key differences: a link between structure, binding specificity and fibrillation enhancement. *J. Am. Chem. Soc.* 128:9893–9901.
37. Chen, M., M. Margittai, …, R. Langen. 2007. Investigation of alpha-synuclein fibril structure by site-directed spin labeling. *J. Biol. Chem.* 282:24970–24979.
38. Del Mar, C., E. A. Greenbaum, …, V. L. Woods, Jr. 2005. Structure and properties of alpha-synuclein and other amyloids determined at the amino acid level. *Proc. Natl. Acad. Sci. USA.* 102:15477–15482.
39. Lamberto, G. R., A. Binolfi, …, C. O. Fernández. 2009. Structural and mechanistic basis behind the inhibitory interaction of PcTS on alpha-synuclein amyloid fibril formation. *Proc. Natl. Acad. Sci. USA.* 106:21057–21062.

Please cite this article in press as: Esteban-Martín et al., Identification of Fibril-Like Tertiary Contacts in Soluble Monomeric α-Synuclein, Biophysical Journal (2013), http://dx.doi.org/10.1016/j.bpj.2013.07.044




40. Giasson, B. I., I. V. Murray, …, V. M. Lee. 2001. A hydrophobic stretch of 12 amino acid residues in the middle of alpha-synuclein is essential for filament assembly. *J. Biol. Chem.* 276:2380–2386.

41. Capaldi, A. P., C. Kleanthous, and S. E. Radford. 2002. Im7 folding mechanism: misfolding on a path to the native state. *Nat. Struct. Biol.* 9:209–216.

42. Korzhnev, D. M., X. Salvatella, …, L. E. Kay. 2004. Low-populated folding intermediates of Fyn SH3 characterized by relaxation dispersion NMR. *Nature.* 430:586–590.

43. Di Nardo, A. A., D. M. Korzhnev, …, A. R. Davidson. 2004. Dramatic acceleration of protein folding by stabilization of a nonnative backbone conformation. *Proc. Natl. Acad. Sci. USA.* 101:7954–7959.

44. Salvatella, X., C. M. Dobson, …, M. Vendruscolo. 2005. Determination of the folding transition states of barnase by using PhiI-value-restrained simulations validated by double mutant PhiIJ-values. *Proc. Natl. Acad. Sci. USA.* 102:12389–12394.

45. Neudecker, P., P. Robustelli, …, L. E. Kay. 2012. Structure of an intermediate state in protein folding and aggregation. *Science.* 336:362–366.

46. Espinoza-Fonseca, L. M. 2012. Aromatic residues link binding and function of intrinsically disordered proteins. *Mol. Biosyst.* 8:237–246.

47. Vendruscolo, M. 2007. Determination of conformationally heterogeneous states of proteins. *Curr. Opin. Struct. Biol.* 17:15–20.

48. Mittag, T., and J. D. Forman-Kay. 2007. Atomic-level characterization of disordered protein ensembles. *Curr. Opin. Struct. Biol.* 17:3–14.

49. Kim, H. Y., M. K. Cho, …, M. Zweckstetter. 2009. Structural properties of pore-forming oligomers of alpha-synuclein. *J. Am. Chem. Soc.* 131:17482–17489.

50. Celej, M. S., R. Sarroukh, …, V. Raussens. 2012. Toxic prefibrillar α-synuclein amyloid oligomers adopt a distinctive antiparallel β-sheet structure. *Biochem. J.* 443:719–726.

51. Jahn, T. R., and S. E. Radford. 2005. The Yin and Yang of protein folding. *FEBS J.* 272:5962–5970.

52. Sandberg, A., L. M. Luheshi, …, T. Härd. 2010. Stabilization of neurotoxic Alzheimer amyloid-beta oligomers by protein engineering. *Proc. Natl. Acad. Sci. USA.* 107:15595–15600.

53. Ehrnhoefer, D. E., J. Bieschke, …, E. E. Wanker. 2008. EGCG redirects amyloidogenic polypeptides into unstructured, off-pathway oligomers. *Nat. Struct. Mol. Biol.* 15:558–566.

54. Roodveldt, C., C. W. Bertoncini, …, C. M. Dobson. 2009. Chaperone proteostasis in Parkinson's disease: stabilization of the Hsp70/alpha-synuclein complex by Hip. *EMBO J.* 28:3758–3770.

55. Lendel, C., C. W. Bertoncini, …, G. Toth. 2009. On the mechanism of nonspecific inhibitors of protein aggregation: dissecting the interactions of alpha-synuclein with Congo red and lacmoid. *Biochemistry.* 48:8322–8334.

56. Yap, T. L., C. M. Pfefferkorn, and J. C. Lee. 2011. Residue-specific fluorescent probes of α-synuclein: detection of early events at the N- and C-termini during fibril assembly. *Biochemistry.* 50:1963–1965.

57. Ahmad, B., Y. Chen, and L. J. Lapidus. 2012. Aggregation of α-synuclein is kinetically controlled by intramolecular diffusion. *Proc. Natl. Acad. Sci. USA.* 109:2336–2341.

58. Schneider, R., J. R. Huang, …, M. Blackledge. 2012. Towards a robust description of intrinsic protein disorder using nuclear magnetic resonance spectroscopy. *Mol. Biosyst.* 8:58–68.

59. Esteban-Martín, S., R. B. Fenwick, and X. Salvatella. 2010. Refinement of ensembles describing unstructured proteins using NMR residual dipolar couplings. *J. Am. Chem. Soc.* 132:4626–4632.

60. Iwahara, J., C. D. Schwieters, and G. M. Clore. 2004. Ensemble approach for NMR structure refinement against (1)H paramagnetic relaxation enhancement data arising from a flexible paramagnetic group attached to a macromolecule. *J. Am. Chem. Soc.* 126:5879–5896.

61. Xue, Y., I. S. Podkorytov, …, N. R. Skrynnikov. 2009. Paramagnetic relaxation enhancements in unfolded proteins: theory and application to drkN SH3 domain. *Protein Sci.* 18:1401–1424.

62. Mukrasch, M. D., S. Bibow, …, M. Zweckstetter. 2009. Structural polymorphism of 441-residue tau at single residue resolution. *PLoS Biol.* 7:e34.

63. Gillespie, J. R., and D. Shortle. 1997. Characterization of long-range structure in the denatured state of staphylococcal nuclease. II. Distance restraints from paramagnetic relaxation and calculation of an ensemble of structures. *J. Mol. Biol.* 268:170–184.

64. Song, J., L. W. Guo, …, J. L. Markley. 2008. Intrinsically disordered gamma-subunit of cGMP phosphodiesterase encodes functionally relevant transient secondary and tertiary structure. *Proc. Natl. Acad. Sci. USA.* 105:1505–1510.